NRC·CNRC

NRC Publications Archive
Archives des publications du CNRC

Permanent magnets with embedded phase changing material for electric motor thermal management

Lamarre, Jean-Michel; Ibrahim, Maged; Pelletier, Roger; Vatandoost, Hossein; Bernier, Fabrice

This publication could be one of several versions: author's original, accepted manuscript or the publisher's version. / La version de cette publication peut être l'une des suivantes : la version prépublication de l'auteur, la version acceptée du manuscrit ou la version de l'éditeur.

For the publisher's version, please access the DOI link below./ Pour consulter la version de l'éditeur, utilisez le lien DOI ci-dessous.

Publisher's version / Version de l'éditeur:

https://doi.org/10.1063/5.0219982

Journal of Applied Physics, 136, 17, pp. 1-8, 2024-11-05

NRC Publications Archive Record / Notice des Archives des publications du CNRC :

https://nrc-publications.canada.ca/eng/view/object/?id=fa1121e9-3f1e-4d24-8fc5-10a3ef292637

https://publications-cnrc.canada.ca/fra/voir/objet/?id=fa1121e9-3f1e-4d24-8fc5-10a3ef292637

Access and use of this website and the material on it are subject to the Terms and Conditions set forth at

https://nrc-publications.canada.ca/eng/copyright

READ THESE TERMS AND CONDITIONS CAREFULLY BEFORE USING THIS WEBSITE.

L'accès à ce site Web et l'utilisation de son contenu sont assujettis aux conditions présentées dans le site

https://publications-cnrc.canada.ca/fra/droits

LISEZ CES CONDITIONS ATTENTIVEMENT AVANT D'UTILISER CE SITE WEB.

Questions? Contact the NRC Publications Archive team at PublicationsArchive-ArchivesPublications@nrc-cnrc.gc.ca. If you wish to email the authors directly, please see the first page of the publication for their contact information.

Vous avez des questions? Nous pouvons vous aider. Pour communiquer directement avec un auteur, consultez la première page de la revue dans laquelle son article a été publié afin de trouver ses coordonnées. Si vous n'arrivez pas à les repérer, communiquez avec nous à PublicationsArchive-ArchivesPublications@nrc-cnrc.gc.ca.

National Research Council Canada | Conseil national de recherches Canada

Canada

Journal of Applied Physics ARTICLE pubs.aip.org/aip/jap

Permanent magnets with embedded phase changing material for electric motor thermal management

Cite as: J. Appl. Phys. **136**, 174901 (2024); doi: 10.1063/5.0219982
Submitted: 21 May 2024 · Accepted: 16 September 2024 ·
Published Online: 5 November 2024

View Online Export Citation CrossMark

Jean-Michel Lamarre,[1,a)] Maged Ibrahim,[2] Roger Pelletier,[1] Hossein Vatandoost,[1] and Fabrice Bernier[1]

AFFILIATIONS

[1]National Research Council Canada, Automotive Research Center, Boucherville, Québec, J4B6Y4, Canada
[2]German International University of Cairo, Administrative Capital, Regional Ring Rd, Cairo Governorate Desert, Cairo, Egypt

Note: This paper is part of the special topic, Phase-change Materials and Their Applications.
[a)]**Author to whom correspondence should be addressed:** jean-michel.lamarre@cnrc-nrc.gc.ca

ABSTRACT

The magnetic performance of NdFeB permanent magnets rapidly decreases as their operation temperature increases. This limits the power output of electric motors as their internal temperature quickly increases with the power demand. This is particularly problematic for applications where high peak power is required for a short period of time, for example during automobile highway acceleration or during an airplane lift-off. With the advances in additive manufacturing, one can envision to fabricate more complex motor geometries and magnetic structures, without additional costs, allowing for enhanced functionalities such as better thermal management. In this context, this paper investigates the feasibility of using phase changing materials (PCMs) to mitigate the temperature rise in permanent magnets (PMs) fabricated by additive manufacturing. The potential of PCM and its relevance was validated by modeling the thermal response of an electric motor during a representative electric vehicle driving scenario. It was found that segmented magnets with embedded phase changing materials would allow to efficiently control temperature rise. To validate the simulation results, PM test pieces with and without embedded PCMs were fabricated using cold spray additive manufacturing and tested using a custom laser thermal cycling setup.

Published under a nonexclusive license by AIP Publishing. https://doi.org/10.1063/5.0219982

31 January 2025 12:47:34

I. INTRODUCTION

Permanent magnet (PM) electric motors are predominant in high performance applications due to their high torque, efficiency, and power density.[1] NdFeB PMs are widely used for this motor type; however, their performance is rapidly decreasing for operating temperatures higher than 100 °C.[2] To prevent demagnetization, heavy rare earth elements such as dysprosium (Dy) or terbium (Tb) are added to NdFeB magnets to increase their coercive force and thus increase their operating temperature limit.[3] For example, a high coercivity NdFeB magnet, containing up to 4% Dy, retains linear magnetization up to a temperature of about 175 °C.[4] However, adding these elements is an expensive solution as heavy rare earths availability is limited. Furthermore, Dy addition is also reducing PM remanence and BH_{max}.[5] Another approach is to limit the magnet temperature increase by using motor cooling. Unfortunately, cooling systems are mostly limited to the stator structure as it is very difficult to route a liquid cooling system to a rotor operating at several thousand rpms. As such, there is usually no direct conductive cooling of the rotor. Rotor cooling is thus limited to inefficient convective or radiative heat transfers with the cooled stator across the airgap.

The use of a phase changing material (PCM) as a thermal management or thermal buffering method to accommodate peak transient loads in vehicle components has been reviewed by Jankowski and McCluskey.[6] More specifically, insertion of solid–liquid PCM, mostly paraffin, was explored to be used in different locations in electric motors, for example in the winding heads,[7] in the casing or housing[8–10] and in hollow conductors.[11,12] Yi and Haran compared different PCMs [paraffin, erythritol, and Ba $(OH)_2 \cdot H_2O$] and showed that depending on the requirements of the application and the desired temperature profiles in the motor,

Published under a nonexclusive license by AIP Publishing

one PCM can be more efficient than the others.[13] Lu *et al.* demonstrated that adding fillers such as halloysite and BN in paraffin leads to forming mechanically stable PCMs.[14] Recently, Broumand *et al.* showed by finite element analysis (FEA) simulation the potential of using PCMs in the stator core of an axial motor.[15] While they mentioned the potential benefits of additive manufacturing (AM) as a mean to fabricate these structures, their paper lacks experimental validation.

Inserting a PCM directly into the rotor structure in order to limit temperature rise brings a different set of advantages to motor design as it could potentially allow to better control the temperature of the rotor, a part of the motor where traditional cooling is more difficult to implement for the previously listed reasons. PCM inclusion in the rotor has not been explored yet as fabricating the required geometry is a challenge. Indeed, as most PCMs are becoming liquid during the phase transition, a retaining structure is required. Inserting PCM in traditional magnets fabricated by compaction is not industrially viable as sintered magnets are difficult to machine and their shape is typically limited to simple geometries rendering the fabrication of structures suitable to accommodate PCMs very difficult. With the advent of AM, it is now possible to build soft magnetic cores and[16,17] and PMs[18–20] with integrated cavities that can readily be used for thermal management purposes.

In this paper, a novel cold spray additive manufacturing methodology was used to fabricate hollow PMs and to integrate phase changing materials to limit temperature rise of the rotor structure. The paper is organized as follows: the choice of PCMs is first described in Sec. II. Section III presents the selected motor structure with high rotor losses and the simulations that were performed to assess the potential of phase changing materials in typical driving cycle conditions. Several arrangements of the phase changing material in the rotor are tested in order to determine the optimal PCM positioning. Finally, Sec. IV presents the fabrication of PM samples with and without PCM using cold spray additive manufacturing. Their performance is assessed by comparison with simulations.

II. SELECTION OF PCM

In order to be used for thermal protection of PMs in electric motor applications, the phase transition temperature of the PCM should fall below the magnet and motor maximum operation temperatures while being significantly above room temperature. In this study, erythritol was selected for demonstration purpose as it satisfies this criterion, is inexpensive and is safe to manipulate. Furthermore, erythritol has a higher latent heat storage capacity than other organic compounds such as paraffin. On the other hand, erythritol is known to undergo an important supercooling which reduces the solidification temperature by several tens of degree, depending on the conditions.[21,22] This could decrease the capacity of erythritol to thermally protect the magnets during the next high-power demand. The erythritol supercooling disadvantages can be mitigated by the use of additives[23,24] or by encapsulation.[25] The main characteristics of erythritol are presented in Table I alongside the thermal properties of aluminum and sprayed magnets that will be presented in a later section.

TABLE I. Thermal properties of erythritol,[12] aluminum, and sprayed NdFeB-Al magnets.

Properties	PCM	Al 6061	Cold spray magnet
Density (kg/m^3)	1450	2700	7500
Solid thermal conductivity [W/(m°C)]	0.5	167	73
Solid specific heat [kJ/(kg °C)]	2.2	0.90	0.55
Liquid specific heat [kJ/(kg °C)]	2.6	…	…
Latent heat (kJ/kg)	319	…	…
Melting point (°C)	118	…	…

III. MAGNETS WITH PCMS IN ELECTRIC MOTORS

Recently, concentrated winding PM synchronous motors have gained increased industrial interest due to their short end-turns, high fault tolerance and the possibility of stator fabrication with high slot fill factors; these can lead to higher reliability and reduced copper losses compared to conventional distributed winding designs. However, one of the main limitations for the wide adoption of this technology is its relatively high rotor losses due to the winding-generated harmonics that are not in synchronism with the rotor.[26] In the present work, a 10-pole/12-slot PM synchronous motor with concentrated windings and interior magnets was designed for an electric vehicle (EV) application to investigate the potential of PCMs in limiting the magnet temperature rise. The simulated motor peak rated power is 55 kW with a base speed of 2800 rpm and a maximum speed of 14 000 rpm. Figure 1 shows a cross-sectional area of the concentrated winding motor.

The motor is first modeled and simulated using 3D electromagnetic FEA using JMAG software. Figure 2(a) shows a vector plot of the magnet eddy currents at 8000 rpm. Due to the skin effect, the eddy currents at a high frequency tend to concentrate toward the magnet sides, thus causing increased loss density, as shown in Fig. 2(b), which could lead to local irreversible demagnetization. The motor temperature distribution is then calculated using a thermal 3D FEA model, where the motor is cooled using water cooling channels integrated in the aluminum casing, as shown in Fig. 3. The copper, iron, and magnet loss distributions in the FEA thermal model are exported from the electromagnetic FEA model.

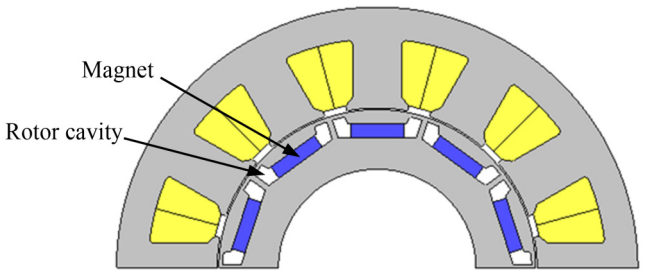

FIG. 1. Structure of a 10-pole 12-slot interior PM motor.

31 January 2025 12:47:34

Published under a nonexclusive license by AIP Publishing

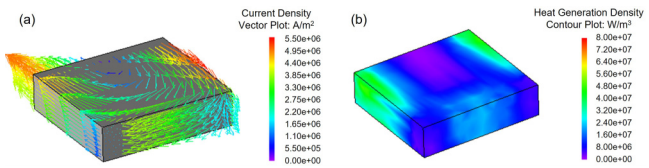

FIG. 2. 3D FEA simulations for (a) magnet eddy current density and (b) magnet loss density.

In order to limit the temperature rise at the magnet sides, the PCM is placed in the rotor cavities shown in Fig. 1. The PCM is modeled by the apparent heat capacity method.[27] Using this method, the PCM specific heat is defined as a piecewise function of temperature, where the specific heat is artificially increased in the temperature interval during which the material state transitions from a solid to liquid. The integral of the specific heat over this transition temperature region is equivalent to the PCM latent heat.

The FEA calculated average temperatures on the side surfaces of the magnets are shown in Fig. 4 before and after placing PCM in the rotor cavities. Near the erythritol melting point (118°), the PCM absorbs a part of the generated heat during its phase transition, thus limiting the magnet side temperature rise. Figure 5 compares the magnet temperature distribution after 15 s of 50 kW transient loading with and without PCMs. While the PCM can effectively reduce the temperature on the magnet sides, it has a relatively lower impact on the average temperature over the whole magnet volume. In addition, only 10.5% of the PCM volume in the cavities is found to be contributing to the magnet temperature regulation, as the remaining PCM volume is still below 118 °C, as illustrated in Fig. 6.

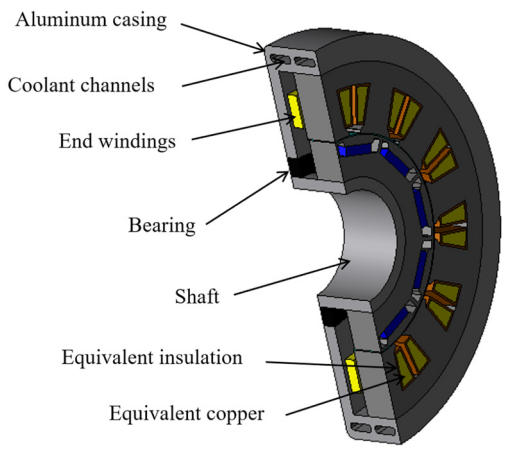

FIG. 3. 3D thermal FEA model of the 10-pole/12-slot indirect liquid-cooled motor.

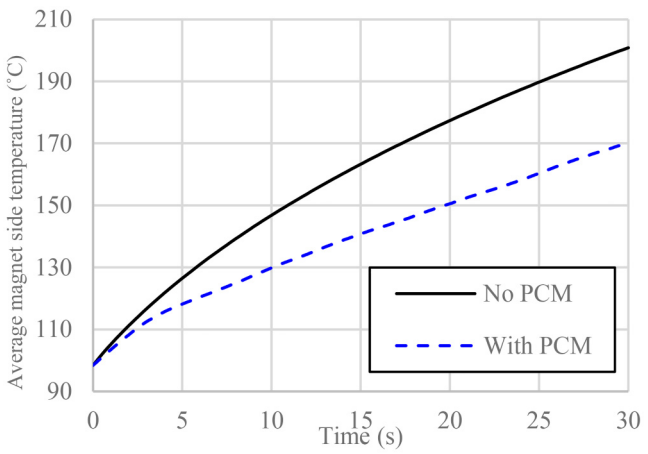

FIG. 4. Comparison of the average magnet side surface temperature with and without PCM.

In order to maximize the contact surface area between the PCM and rotor magnets, each magnet is then segmented into three and six segments with PCM placed in gaps between the magnets, as shown in the rotor designs in Fig. 7. To ensure a fair comparison of the designs, the total magnet volume was kept constant, maintaining similar magnetic loading across all designs. Since each design uses the same stator and armature current magnitude, the magnet segmentation results in only a minor change in output torque (<2%), which can be compensated through design optimization. Also, all the designs utilize a similar total PCM volume. It should be noted that while magnet segmentation in PM machines generally leads to a reduction in the magnet eddy current loss,[28] it is assumed throughout the simulations that all the designs have the same magnet loss density to evaluate only the thermal impact of the PCM position. The simulated temperature distribution in Fig. 8 shows a higher PCM effectiveness with the three and six segmented magnets during the transient stage as the increased PCM/magnet interface area improves the extraction of magnet-generated heat during the phase changing period. This is also reflected in the transient average magnet temperature, shown in Fig. 9, where the three and six segment designs can increase the allowable transient time before reaching a magnet average temperature of 150 °C by 232%

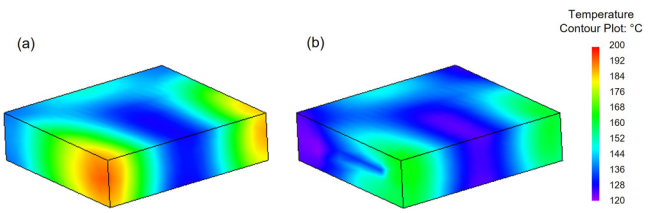

FIG. 5. Magnet temperature distribution after 15 s of 50 kW transient loading (a) without PCM and (b) with PCM.

31 January 2025 12:47:34

Published under a nonexclusive license by AIP Publishing

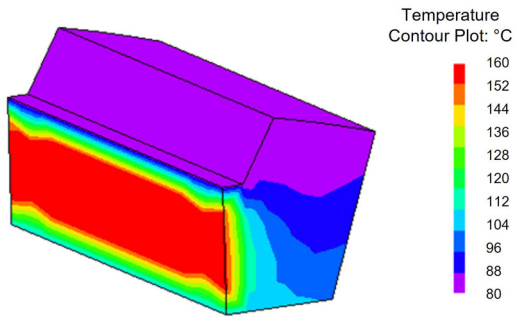

FIG. 6. Temperature distribution of the PCM after 15 s of 50 kW transient loading.

and 352%, respectively, compared to the original design with no PCM.

While the segmented design shows good performance, positioning and assembling the magnets within this structure while containing the PCM might be unpractical. Therefore, in addition to the segmented designs, permanent magnets with integrated PCM-filled cavities as shown in Fig. 10 were also investigated. This approach offers the added benefit of increasing the PCM/magnet interface area. Such a configuration can be enabled by additive manufacturing and can achieve significant practical advantages, as the enclosing of the PCM material can prevent leakage issues during operation. More details will be given in Sec. IV. An electric motor with PCM integrated magnets is simulated and compared to a segmented magnet design with similar magnet and PCM volumes. The transient simulation in Fig. 11 shows equivalent temperature rise for both configurations hence indicating that the filled cavity structure would offer suitable performance.

The PM motor with PCM-filled channels is also simulated with varying channel widths (Wc), as illustrated in Fig. 10. The channels are designed with a narrow shape so that a large surface area on the sides would be in parallel with the magnet flux line in order to minimize the obstruction of magnet flux. The motor is first analyzed using 2D electromagnetic FEA with different magnet widths. The average torque for each design is shown in Fig. 12. The transient thermal behavior for each motor is then simulated using 3D thermal FEA. The electromagnetic and thermal results in Fig. 12 show that increasing the PCM channel thickness beyond 1 mm causes a significant reduction in the motor average torque

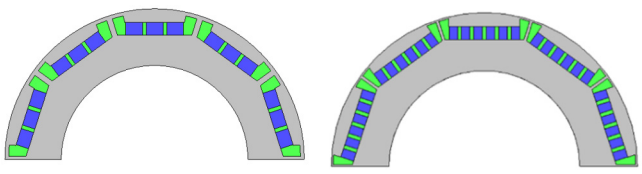

FIG. 7. PM rotor designs with (a) three magnet segments and (b) six magnet segments. Magnets and PCM are colored blue and green, respectively.

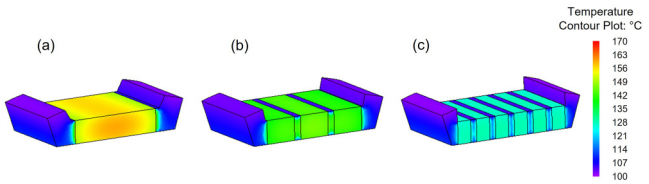

FIG. 8. Magnet temperature distribution after 90 s of transient condition for (a) one magnet segment, (b) three magnet segments, and (c) six magnet segments.

due to decreased effective magnet flux. On the other hand, narrower channels result in a smaller degradation of the electromagnetic performance, for example 0.8 mm PCM channels reduce the average torque by about 5%. On the other hand, these 0.8 mm channels extend the transient time for the average magnet temperature to reach 130 °C by 45% compared to a solid magnet without PCM.

A PM motor equipped with five 0.8 mm channels filled with erythritol is then compared to the baseline motor with solid permanent magnets, using electromagnetic and thermal FEA simulations. Table II compares the operating conditions and electromagnetic performance of the two motors. The PM motor with PCM-filled channels exhibits a reduced magnet volume, leading to a lower magnetic loading. In order to reach the same average torque of the baseline design, its armature current is increased by 4%, which, in turn, raises both the armature copper losses and magnet losses, as detailed in Table I. The copper, iron, and magnet losses, calculated from the electromagnetic FEA models, are then used as inputs for 3D thermal FEA models to assess the transient thermal characteristics of the motors. Figure 13 illustrates the transient average temperatures for the armature coils and permanent magnets of the two motors. Although the motor with PCM has higher losses, resulting in increased average copper temperatures and a slight rise in initial

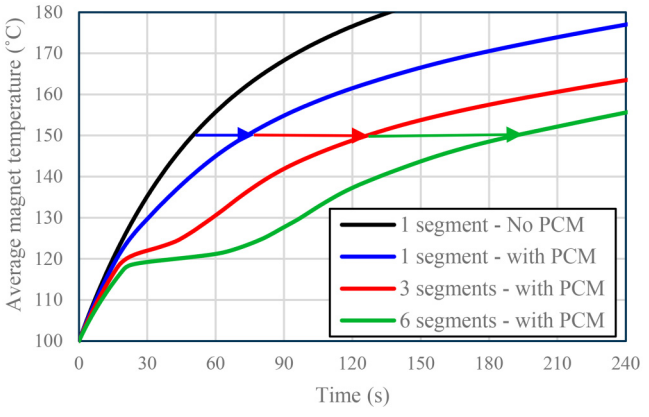

FIG. 9. Thermal transient analysis with different magnet/PCM configurations at 50 kW/8000 rpm.

31 January 2025 12:47:34

Published under a nonexclusive license by AIP Publishing

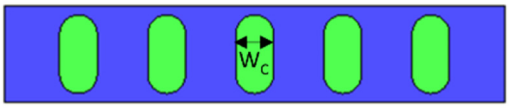

FIG. 10. Cross-sectional area of permanent magnet with PCM-filled cavities.

magnet temperatures, the erythritol's phase change process mitigates the magnet temperature rise once it reaches its melting point. This extends the allowable transient operation time before reaching temperatures that could cause irreversible demagnetization of the permanent magnets. It is also important to note that the effectiveness of PCM in PM motors is dependent on the motor operating conditions, particularly its loss density levels. Future research should therefore investigate how motor design, ratings, and operating conditions influence PCM effectiveness.

In order to further assess the performance of the PCM in the context of EV electric motor, a PM motor with PCM integrated channels is simulated and compared to the original design with no PCM under a typical EV operating condition. In the considered scenario, the EV first operates at constant speed for one hour with a motor speed of 8000 rpm and output power of 7 kW. It then accelerates for 1 min with a 50 kW power and afterward returns to the constant speed operation. This scenario can correspond, for example, to a brief acceleration phase of an EV on a highway travel. During this period, the motor losses and temperature distribution are calculated using coupled electromagnetic/thermal FEA models. Figure 14 compares the simulated average magnet temperature with solid magnets and with PCM-filled magnets. The results show that the PCM can reduce the magnet temperature by more than 31 °C.

The demonstrated reduction of the maximum temperature can lead to several motor performance improvements or cost reduction scenarios; for example: (1) The maximum temperature reduction can translate into the use of cheaper magnet grades that

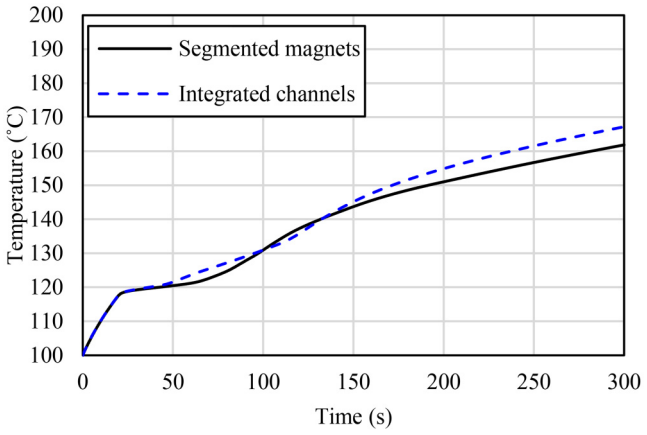

FIG. 11. Comparison of average magnet transient temperature with PCM segmented magnets and PCM integrated magnets.

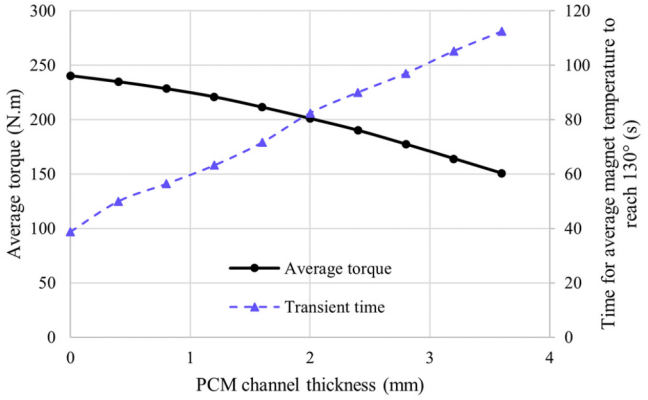

FIG. 12. Effect of PCM channel width on the average torque and transient thermal characteristics of the magnet.

are stable at lower operation temperatures thus allowing to reduce the total motor cost. (2) The PCM can be used in combination with higher coil current to improve the motor peak power output while maintaining the maximum magnet temperature constant. (3) The PCM can be used to allow positioning the magnets in different configurations to improve a specific motor characteristic. (4) The PCM can be used as a motor built-in safety feature to prevent magnet temperature overshoot and demagnetization. Such a safety feature would be available when the PCM is in its solid-state form. When the PCM is melted during a transient condition, the EV drive system should limit sudden power demands during a pre-programmed period (about 80 s for the simulated design) until the PCM solidifies again.

IV. DEMONSTRATION PART FABRICATION

The performed simulations suggest that hollow cavities embedded in PMs (see Fig. 10) can successfully limit magnet

TABLE II. Comparison between PM motors with and without PCM-filled channels.

	PM motor without PCM	PM motor with PCM integrated magnets
Stator winding	Double layer fractional concentrated winding with 14 turns per coil	
Magnet volume (mm^3)	129 500	122 240
Operating speed (rpm)	2400	
Average torque (N m)	100	
Armature current (A)	100.98	105.01
Copper loss (W)	391.53	423.41
Stator iron loss (W)	148.25	148.39
Rotor iron loss (W)	25.13	26.47
Magnet loss (W)	596.32	637.77
Total losses (W)	1161.23	1236.04
Efficiency (%)	95.58	95.31

31 January 2025 12:47:34

Published under a nonexclusive license by AIP Publishing

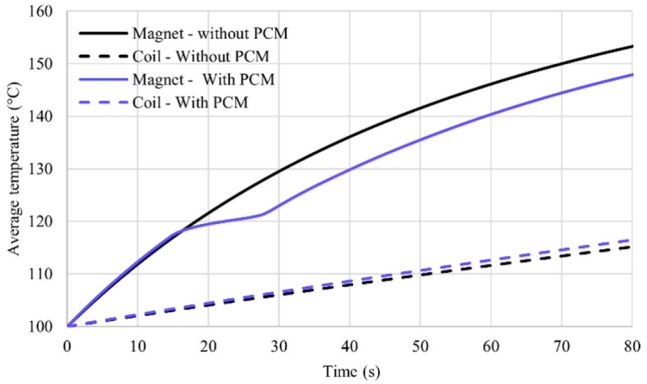

FIG. 13. Transient temperature for PM motors with and without PCM calculated using thermal 3D FEA at 100 N m–2400 rpm.

temperature increase in the EV motor. In the next section of the paper, the fabrication and performance validation of NdFeB PMs prepared by cold spray additive manufacturing is presented. A simple geometry comprising three cavities was selected for demonstration purposes as shown in Fig. 15. The permanent magnets were fabricated by cold spray using a mix of two powders: MQFP-B NdFeB powder from Magnequench and H5 aluminum powder from Valimet. Samples were sprayed onto aluminum 6061 substrates using Plasma Giken PCS800 cold spray gun operating at a gas temperature of 600 °C and a gas pressure of 4.9 MPa. The gun was mounted on a robotic arm and moved at a speed of 100 mm/s relative to the substrate with 1 mm steps. The spray distance was kept at a constant 80 mm. More details on the magnet fabrication procedure as well as on their magnetic properties can be found in Ref. 18. The test pieces dimensions are the following: length = 36.7

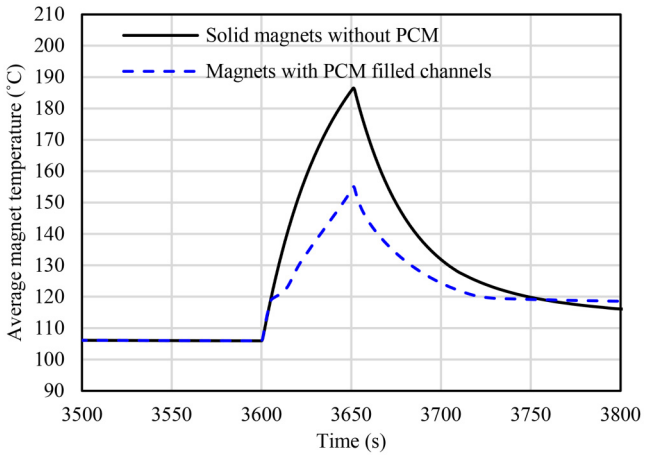

FIG. 14. Magnet average temperature during highway acceleration with and without PCM.

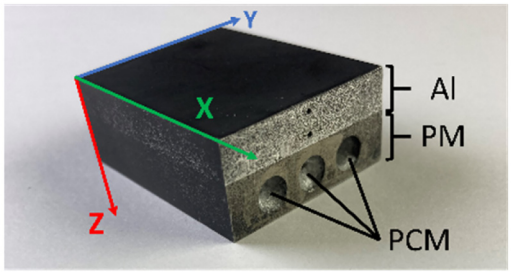

FIG. 15. An aluminum substrate was sprayed with a composite NdFeB-Al magnet. Holes were machined to insert erythritol (PCM).

mm, width = 28.9 mm, thickness of aluminum = 6.1 mm, thickness of magnet = 8.3 mm. Test pieces surface were machined to final dimensions while holes to insert erythritol and thermocouples were drilled using conventional machining. The three cavities were completely filled with a total of 2.32 g of liquid erythritol that was solidified prior to thermal testing. A test pieces without cavities and therefore, without erythritol was also prepared and used as a reference. Further work would be required before motor fabrication to identify a complete methodology that is suitable for production as no method is presented here to seal the cavities.

A custom laser rig setup, shown in Fig. 16, was used to emulate the thermal service conditions a PCM-filled magnet would encounter during a peak demand scenario. The setup allows for efficient, clean, rapid, and safe control of the desired power input. The setup is composed of a 3 kW CO_2 laser, two low temperature ultra-fast response optical pyrometers (OPTRIX, model CT 4ML), a specimen holder and a thermal camera (Jenoptik, model IR-TCM

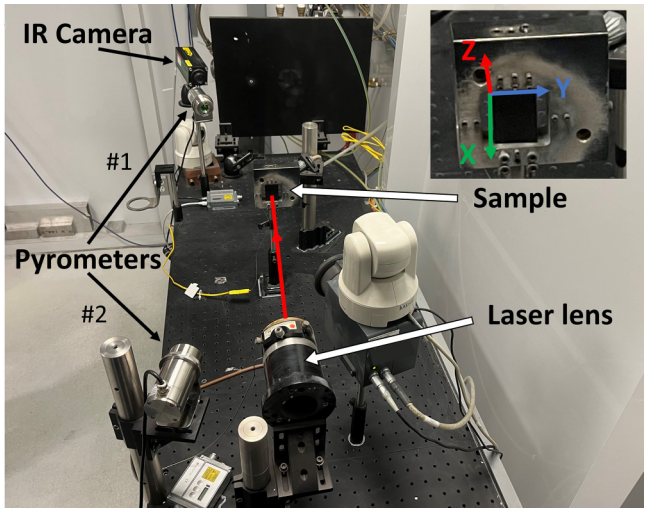

FIG. 16. A custom laser rig was used to thermally cycle the PM samples. The setup is equipped with two optical pyrometers and an IR-camera.

31 January 2025 12:47:34

Published under a nonexclusive license by AIP Publishing

384) and is fully computer controlled. Test pieces with and without PCM were thermally cycled using the laser rig. To ease temperature measurement using the optical pyrometers, the aluminum substrate surface (X–Y plane in Fig. 15) and the opposite surface were painted with a black high emissivity paint. The two test pieces, with and without PCM, were submitted to the laser beam with a power of 50 W until reaching a temperature of 180 °C and then the laser power was switched off to cool down via normal convection and radiation. The selected temperature of 180 °C is above the erythritol melting point as well as being slightly above the typical operation temperature of NdFeB magnets. The laser spot diameter was 25 mm. The temperature at the center of the hot and cold faces were recorded at a rate of 10 Hz using optical pyrometers labeled as pyrometer 1 and pyrometer 2, respectively, in Fig. 16.

The experimental results were compared to a digital twin simulation performed by FEA using material thermal parameters. Thermal properties of erythritol, aluminum, and NdFeB used in the numerical simulations are reported in Table I. The aim is to validate the experimental performance of the PCM and the ability to correctly predict numerically the performance of a real-life system. As before, the PCM was again modeled by the apparent heat capacity method. In order to replicate more closely the experimental conditions in the FEA simulations, the apparent heat transfer coefficient at the test pieces outer surfaces was determined by matching the measured temperature during the cooling period. A value of 10 W/(m^2 °C) was found, which falls at the upper limit of the spectrum for natural convection of a vertical wall.[29] The effective heating laser power was extracted using a similar strategy by matching the aluminum temperature rise of the heated face during the initial heating period.

Figure 17 shows the measured and simulated temperatures at the magnet surface for the PMs with and without PCM for a typical cycle. An excellent agreement was observed between the measured and simulated data for both kinds of samples. Figure 17 further shows that before the melting temperature of the PCM (118 °C) is reached, the surface temperature of the magnet is essentially the same in the two configurations. After this moment, the melting of the PCM slows down the heating rate of the magnet. This different heating rate would continue until the PCM is completely melted. It is worth nothing that the PCM is not completely melted as can be seen by the slope of the temperature increase. In this particular example, the presence of the PCM led to a considerable decrease of 20 °C of the peak temperature. These sets of results, physical and numerical, clearly confirm the PCM capability of limiting the magnet temperature increase.

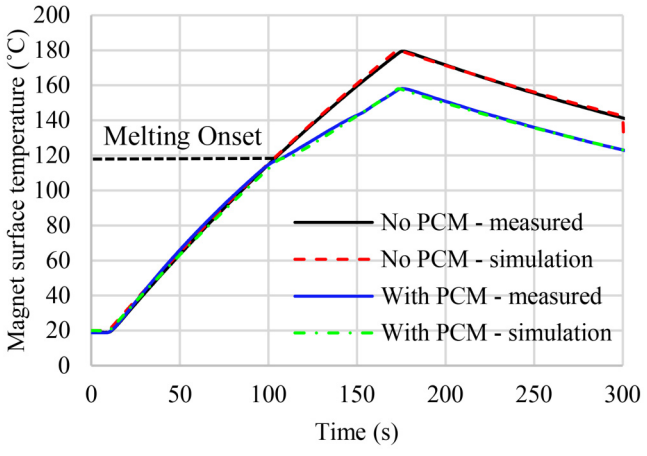

FIG. 17. Comparison of the measured and simulated magnet surface temperatures with and without PCM.

V. CONCLUSIONS

The use of PCM materials was explored to control the temperature rise of PMs in an EV application. FEA simulations have demonstrated that erythritol is a suitable material for that application. The use of PCMs in a PM synchronous motor with concentrated windings was simulated illustrating the potential of PCMs for magnet temperature control in electric motors. Simulations have further shown that segmented and cavity structures are suitable configurations to optimize PCM usage via more complete melting. The cavity-based structure was selected for its ease of fabrication using additive manufacturing. Permanent magnets were fabricated using cold spray deposition and the PCM was inserted in machined cavities. The thermal performance of PCM-inserted magnets matched the prediction from numerical simulations. Results are promising for cost reduction of magnets in electric motors, increase power level, geometrical flexibility, or as built-in safety features.

ACKNOWLEDGMENTS

Crown Copyright ©2024. His Majesty the King in Right of Canada, as represented by the National Research Council, Canada.

AUTHOR DECLARATIONS

Conflict of Interest

The authors have no conflicts to disclose.

Author Contributions

Jean-Michel Lamarre: Conceptualization (lead); Data curation (equal); Formal analysis (lead); Funding acquisition (lead); Investigation (equal); Methodology (equal); Project administration (lead); Resources (lead); Supervision (lead); Validation (equal); Writing – original draft (equal); Writing – review & editing (lead). **Maged Ibrahim:** Data curation (equal); Formal analysis (equal); Investigation (equal); Methodology (equal); Software (lead); Validation (equal); Writing – original draft (equal). **Roger Pelletier:** Data curation (equal); Formal analysis (equal); Investigation (supporting); Methodology (supporting); Writing – original draft (supporting). **Hossein Vatandoost:** Data curation (supporting); Software (supporting); Visualization (supporting); Writing – review & editing (supporting). **Fabrice Bernier:** Conceptualization (equal); Formal analysis (equal); Funding acquisition (equal); Investigation (equal); Project administration (equal); Visualization (equal); Writing – review & editing (equal).

31 January 2025 12:47:34

Published under a nonexclusive license by AIP Publishing

DATA AVAILABILITY

The data that support the findings of this study are available from the corresponding author upon reasonable request.

REFERENCES

[1]A. Vagati, A. Fratta, G. Franceschini, and P. Rosso, "AC motors for high-performance drives: A design-based comparison," IEEE Trans. Ind. Appl. **32**(5), 1211–1219 (1996).

[2]M. S. Walmer, C. H. Chen, and M. H. Walmer, "A new class of Sm-TM magnets for operating temperatures up to 550/spl deg/C," IEEE Trans. Magn. **36**(5), 3376–3381 (2000).

[3]C. C. Pavel, C. Thiel, S. Degreif, D. Blagoeva, M. Buchert, D. Schüler, and E. Tzimas, "Role of substitution in mitigating the supply pressure of rare earths in electric road transport applications," Sustain. Mater. Technol. **12**, 62–72 (2017).

[4]O. Gutfleisch, M. A. Willard, E. Brück, C. H. Chen, S. G. Sankar, and J. P. Liu, "Magnetic materials and devices for the 21st century: Stronger, lighter, and more energy efficient," Adv. Mater. **23**(7), 821–842 (2011).

[5]M. Hirota, M. Sanada, S. Morimoto, and Y. Inoue, "Improvement of rotor structure on irreversible demagnetization in double-layered IPMSM with Dy-less magnet," in *2015 IEEE Energy Conversion Congress and Exposition (ECCE)* (IEEE, 2015), pp. 1795–1802.

[6]N. R. Jankowski and F. P. McCluskey, "A review of phase change materials for vehicle component thermal buffering," Appl. Energy **113**, 1525–1561 (2014).

[7]J. Bellettre, V. Sartre, F. Biais, and A. Lallemand, "Transient state study of electric motor heating and phase change solid-liquid cooling," Appl. Therm. Eng. **17**(1), 17–31 (1997).

[8]S. Wang, Y. Li, Y.-Z. Li, J. Wang, X. Xiao, and W. Guo, "Transient cooling effect analyses for a permanent-magnet synchronous motor with phase-change-material packaging," Appl. Therm. Eng. **109**, 251–260 (2016).

[9]S. Wang, Y.-Z. Li, Y. Liu, H. Zhou, Y. Li, W. Guo, and X. Xiao, "Temperature control of permanent-magnet synchronous motor using phase change material," in *2015 IEEE International Conference on Advanced Intelligent Mechatronics* (IEEE, 2015), pp. 1635–1640.

[10]J.-X. Wang, Y. Z. Li, S.-N. Wang, H.-S. Zhang, X. Ning, and W. Guo, "Experimental investigation of the thermal control effects of phase change material based packaging strategy for on-board permanent magnet synchronous motors," Energy Convers. Manage. **123**, 232–242 (2016).

[11]S. Ayat, B. Dagusé, and R. Khazaka, "Design considerations of windings formed with hollow conductors cooled with phase change material," in *2019 IEEE Energy Conversion Congress and Exposition* (IEEE, 2019), pp. 5652–5658.

[12]S. Ayat, C. Serghine, T. Klonowski, S. Yon, A. Mutabazi, and S. McDaniel, "The use of phase change material for the cooling of electric machine windings formed with hollow conductors," *2019 IEEE International Electric Machines & Drives Conference* (IEEE, 2019), pp. 1195–1201.

[13]X. Yi and K. S. Haran, "Transient performance study of high-specific-power motor integrated with phase change material for transportation electrification," *2020 IEEE Transportation Electrification Conference & Expo* (IEEE, 2020), pp. 119–124.

[14]M. Lu, X. Wang, and L. Liu, "Form-stable composite phase change material based cooling of small brushless DC motor windings," IEEE Trans. Compon. Packag. Manuf. Technol. **13**(9), 1410–1420 (2023).

[15]M. Broumand, S. Yun, and Z. Hong, "A novel phase change material-based thermal management of electric machine windings enabled by additive manufacturing," Appl. Therm. Eng. **244**, 122802 (2024).

[16]A. Plotkowski, K. Carver, F. List, J. Pries, Z. Li, A. M. Rossy, and D. Leonard, "Design and performance of an additively manufactured high-Si transformer core," Mater. Des. **194**, 108894 (2020).

[17]F. N. U. Nishanth, A. D. Goodall, I. Todd, and E. L. Severson, "Characterization of an axial flux machine With an additively manufactured stator," IEEE Trans. Energy Convers. **38**(4), 2717–2729 (2023).

[18]J.-M. Lamarre and F. Bernier, "Permanent magnets produced by cold spray additive manufacturing for electric engines," J. Therm. Spray Technol. **28**(7), 1709–1717 (2019).

[19]J.-M. Lamarre and F. Bernier, Methods of manufacturing permanent magnets by additive manufacturing, U.S.20230005649A1 (5 January 2023).

[20]H. Wang, T. N. Lamichhane, and M. P. Paranthaman, "Review of additive manufacturing of permanent magnets for electrical machines: A prospective on wind turbine," Mater. Today Phys. **24**, 100675 (2022).

[21]M. Osei, O. Staveland, S. McGowan, J. B. Unger, N. R. Christler, M. Weeman, M. E. Strutz, M. Walker, M. B. Maun, N. C. Dunning, M. M. Bekheit, J. C. P. Abraham, L. Cox, G. Gius, O. Hansel, E. O. Amoafo, N. Hugo, and P. Schwartz, "Phase change thermal storage: Cooking with more power and versatility," Sol. Energy **220**, 1065–1073 (2021).

[22]T. Adachi, D. Daudah, and G. Tanaka, "Effects of supercooling degree and specimen size on supercooling duration of erythritol," ISIJ Int. **54**(12), 2790–2795 (2014).

[23]J.-L. Zeng, L. Zhou, Y.-F. Zhang, S.-L. Sun, Y.-H. Chen, L. Shu, L.-P. Yu, L. Zhu, L.-B. Song, and Z. Cao, "Effects of some nucleating agents on the supercooling of erythritol to be applied as phase change material," J. Therm. Anal. Calorim. **129**(3), 1291 (2017).

[24]X.-F. Shao, S. Yang, J.-C. Lin, H.-R. Teng, L.-W. Fan, J. N. Chiu, Y.-P. Yuan, and V. Martin, "Polyvinylpyrrolidone (PVP)-enabled significant suppression of supercooling of erythritol for medium-temperature thermal energy storage," J. Energy Storage **46**, 103915 (2022).

[25]Y. Wang, S. Li, T. Zhang, D. Zhang, and H. Ji, "Supercooling suppression and thermal behavior improvement of erythritol as phase change material for thermal energy storage," Sol. Energy Mater. Sol. Cells **171**, 60–71 (2017).

[26]A. M. EL-Refaie, "Fractional-slot concentrated-windings synchronous permanent magnet machines: Opportunities and challenges," IEEE Trans. Ind. Electron. **57**(1), 107–121 (2010).

[27]E. M. Alawadhi and C. H. Amon, "PCM thermal control unit for portable electronic devices: Experimental and numerical studies," IEEE Trans. Compon. Packag. Manuf. Technol. **26**(1), 116–125 (2003).

[28]S. Niu, S. L. Ho, W. N. Fu, and J. Zhu, "Eddy current reduction in high-speed machines and eddy current loss analysis with multislice time-stepping finite-element method," IEEE Trans. Magn. **48**(2), 1007–1010 (2012).

[29]M. Popescu, D. A. Staton, A. Boglietti, A. Cavagnino, D. Hawkins, and J. Goss, "Modern heat extraction systems for power traction machines—A review," IEEE Trans. Ind. Appl. **52**(3), 2167–2175 (2016).

31 January 2025 12:47:34

Published under a nonexclusive license by AIP Publishing